references, see Thomlinson & Williams, 1984; Brown & Lindau, 1986).

A position-sensitive detector can replace the receiving slit when a reciprocal space is scanned. TV area detectors with an X-ray-to-visible light converter and two-dimensional CCD arrays have moderate resolution and efficiency, but they work in the current mode and do not provide pulse discrimination on the basis of the photon energy. One- and two-dimensional proportional chambers have a spatial resolution of the order of 0.1 mm, and the relative energy resolution, $\Delta E/E \simeq 0.2$, is sufficient for rejection of some of the parasitic scattering.

The NaI(Tl) scintillation counter is used most frequently as the X-ray detector in crystallography. It has 100% efficiency for the commonly used wavelengths, and the energy resolution is comparable to that of a proportional counter. The detector has a long life, and the level of the low-energy noise can be reduced to about 0.1 counts s^{-1}.

The Ge and Si(Li) solid-state detectors (SSD) have an energy resolution $\Delta E/E = 0.01$ to 0.03 for the wavelengths used in crystallography. The relative Compton shift, $\Delta\lambda/\lambda$, is $(0.024\ \text{Å}/\lambda) \times (1 - \cos 2\theta)$, where 2θ is the scattering angle, so that even this component can be eliminated to some extent by a SSD. These detectors have been bulky and expensive, but new constructions that are suitable for X-ray diffraction have become available recently. The effects of the detector resolution are shown schematically in Fig. 7.4.4.5 for a scintillation counter and a SSD.

Crystal monochromators placed in front of the detector eliminate all inelastic scattering but the TDS. The monochromator must be matched with the preceding X-ray optical system, the sample included, and therefore diffracted-beam monochromators are used in powder diffraction only (see Subsection 7.4.4.4).

7.4.4.4. *Powder diffraction*

The signal-to-background ratio is much worse in powder diffraction than in single-crystal diffraction, because the background is proportional to the irradiated volume in both cases, but the powder reflection is distributed over a ring of which only the order of 1% is recorded. The phase-space diagrams of a typical measurement are shown in Fig. 7.4.4.6. The Johansson monochromator is matched to the incident beam to provide

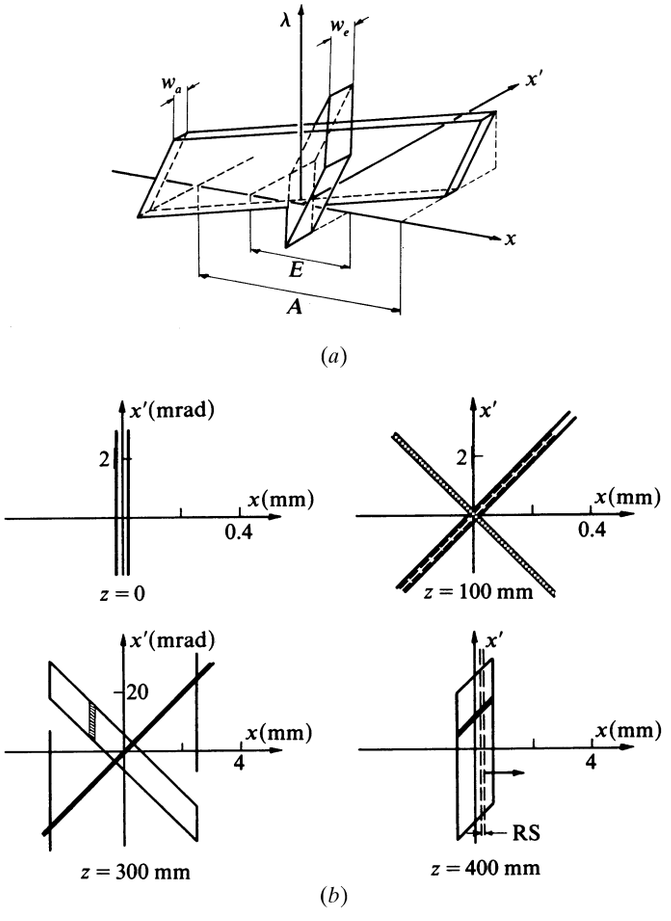

Fig. 7.4.4.6. Equatorial phase-space diagrams for powder diffraction in the Bragg–Brentano geometry. (*a*) The acceptance and emittance windows of a Johannson monochromator; (*b*) the beam in the $\lambda = \lambda_1$ plane: the exit beam from the Johansson monochromator is shown by the hatched area ($z = 100$ mm), the beam on the sample by two closely spaced lines, the reflectivity range of powder particles in a small area of the sample by the hatched area ($z = 300$ mm, note the change of scales), and the scan of the reflected beam by a slit RS by broken lines ($z = 400$ mm, at the parafocus).

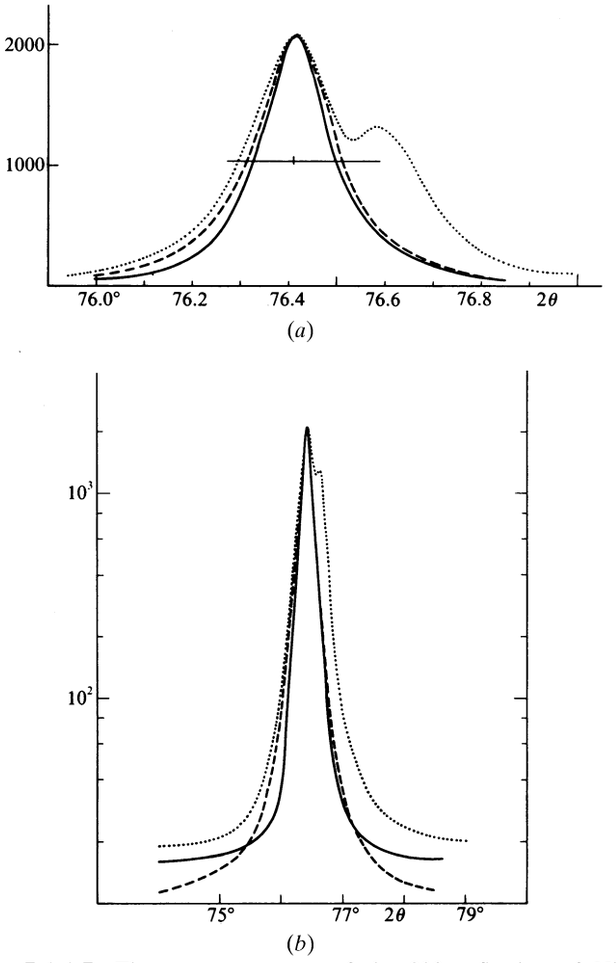

Fig. 7.4.4.7. Three measurements of the 220 reflection of Ni at $\lambda = 1.541$ Å scaled to the same peak value; (*a*) in linear scale, (*b*) in logarithmic scale. Dotted curve: graphite (00.2) Johann monochromator, conventional 0.1 mm wide X-ray source (Suortti & Jennings, 1977); solid curve: quartz (10.1) Johansson monochromator, conventional 0.05 mm wide X-ray source; broken curve: synchrotron radiation monochromatized by a (+, −) pair of Si (111) crystals, where the second crystal is sagittally bent for horizontal focusing (Suortti, Hastings & Cox, 1985). The horizontal line indicates the half-maximum value. In all cases, the effective slit width is much less than the FWHM of the reflection.

maximum flux and good energy resolution. The Bragg–Brentano geometry is parafocusing, and, if the geometrical aberrations are ignored, the reflected beam is a convolution between the angular width of the monochromator focus (as seen from the sample) and the reflectivity curve of an average crystallite of the powder sample. The profile of this function is scanned by a narrow slit, as shown in the last diagram. The slit can be followed with a Johann or Johansson monochromator that has a narrow wavelength pass-band. In this case, there is no primary-beam monochromator, so that the incident beam at the sample is that given at $z = 100$ mm. The slit RS is the 'source' for the monochromator, which focuses the beam at the detector. The obvious advantages of this arrangement are counterbalanced by certain limitations such as that the effective receiving slit is determined by the reflectivity curve of the monochromator, and this may vary over the effective area.

Examples of a powder reflection measured with different instruments and 1.5 Å radiation are given in Fig. 7.4.4.7. It should be noticed that scattering from the impurities of the sample and from the sample environment is negligible in all three cases. The width of the mosaic distribution of the 00.2 reflection of the pyrolytic graphite monochromator is 0.3°, which corresponds to a 180 eV (0.034 Å) wide transmitted beam. This is almost 10 times the separation between $K\alpha_1$ and $K\alpha_2$, and 70 times the natural width of the $K\alpha_1$ line. The width of the focal line is about 0.2 mm, or 0.07°, and is seen as broadening of the reflection profile. The quartz (10.1) monochromator reflects a band that is determined by the projected width of the X-ray source. In the present case, the band is 15 eV wide, so that the monochromator can be tuned to transmit the $K\alpha_1$ component only. The focal line is very sharp, 0.05 mm wide, and so the reflection is much narrower than in the preceding case. The third measurement was made with synchrotron radiation, and the receiving slit was replaced by a perfect-crystal analyser. The divergences of the incident and diffracted beams are about 0.1 mrad (less than 0.01°) in the plane of diffraction, so that the ideal parallel-beam geometry should prevail. However, the reflection is clearly broader than that measured with the conventional diffractometer. The reason is a wavelength gradient across the beam, which was monochromatized by a flat perfect crystal. On the other hand, the Ge (111) analyser crystal transmits elastic scattering and TDS only, and 2° away from the peak the background is 0.5% of the maximum intensity.

The above considerations may seem to have little relevance to everyday crystallographic practices. Unfortunately, many standard methods yield diffraction patterns of poor quality. The quest for maximum integrated intensity has led to designs that make reflections broad and background high. It should be realized that not the flux but the brilliance of the incident beam is important in a diffraction measurement. The other aspect is that the information should not be lost in the experiment, and a divergent wide wavelength band is quite an ignorant probe of a reflection from a single crystal.

A situation where even small departures from the ideal diffraction geometry may cause large effects is measurement at an energy just below an absorption edge. Even a small tail of the energy band of the incident beam may excite radiation that becomes the dominant component of background. Similar effects are due to the harmonic energy bands reflected by most monochromators, particularly when the continuous spectrum of synchrotron radiation is used.

Scattering from the surroundings of the sample can be eliminated almost totally by shielding and beam tunnels. The general idea of the construction should be that an optical element of the instrument 'sees' the preceding element only. Inevitably, the detector sees some of the environment of the sample. The density of air is about 1/1000 of that of a solid sample, so that 10 mm^3 of irradiated air contributes to the background as much as a spherical crystal of 0.3 mm diameter. Strong spurious peaks may arise from slit edges and entrance windows of the specimen chamber, which should never be seen by the detector. A complete measurement without the sample is always a good starting point for an experiment.